Talanta 82 (2010) 325–332

Contents lists available at ScienceDirect

Talanta

journal homepage: www.elsevier.com/locate/talanta

# Spectrofluorimetry in organized media coupled to second-order multivariate calibration for the determination of galantamine in the presence of uncalibrated interferences

María J. Culzoni[a], Ricardo Q. Aucelio[b], Graciela M. Escandar[a,*]

[a] Instituto de Química Rosario (CONICET-UNR), Facultad de Ciencias Bioquímicas y Farmacéuticas, Universidad Nacional de Rosario, Suipacha 531, 2000 Rosario, Argentina
[b] Chemistry Department, Pontifícia Universidade Católica do Rio de Janeiro (PUC-RIO), Rio de Janeiro, RJ 22453-900, Brazil

ARTICLE INFO

*Article history:*
Received 1 March 2010
Received in revised form 15 April 2010
Accepted 17 April 2010
Available online 24 April 2010

*Keywords:*
Spectrofluorimetry
Organized media
Multivariate calibration
Galantamine

ABSTRACT

The present article describes the spectrofluorimetric determination of galantamine, a widely used acetylcholinesterase inhibitor, through excitation–emission fluorescence matrices and second-order calibration. With the purpose of enhancing the fluorescence intensity of this substance, the effect of different organized assemblies was evaluated. Although the interaction of galantamine with different cyclodextrins is weak, it was corroborated that the fluorescence intensity of this pharmaceutical in the presence of α-cyclodextrin is increased by a twofold factor. Among the studied micellar media, the anionic surfactant sodium dodecyl sulfate produced the largest signals for the compound of interest (sixfold enhancement), and was selected as auxiliary reagent for the subsequent determinations. The developed approach enabled the determination of galantamine at the ng mL$^{-1}$ level without the necessity of applying separation steps, and in the presence of uncalibrated interferences. The applied second-order chemometric tools were parallel factor analysis (PARAFAC), unfolded partial least-squares coupled to residual bilinearization (U-PLS/RBL), and multidimensional partial least-squares coupled to residual bilinearization (N-PLS/RBL). The ability of U-PLS/RBL to successfully overcome spectral interference problems is demonstrated. The quality of the proposed method was established with the determination of galantamine in both artificial and natural water samples.



## 1. Introduction

Galantamine (GAL, Fig. 1) is a competitive acetylcholinesterase inhibitor approved for the treatment of mild to moderate Alzheimer's disease [1]. After its oral administration, unchanged GAL and its metabolites are predominantly excreted (93%) by urine [2]. Since this pharmaceutical is administered to patients with chronic treatments during long periods of time, GAL unavoidably reaches the environment through sewage, constituting an emerging contaminant [3,4].

Although in water compartments pharmaceuticals are generally present at rather low levels ranging from ng L$^{-1}$ to μg L$^{-1}$ [5,6], their continuous input may lead to high long-term concentrations, which may promote adverse effects on wildlife and humans.

GAL has been determined in biological, pharmaceutical and plant samples by different methods, including a spectrophotometric procedure followed for inhibition studies of acetylcholinesterase [7], liquid and gas chromatographies [2–15] and capillary electrophoresis [15–17]. While GAL fluorescence detection has been used in some chromatographic methods [2,12], to the extent of our literature search, a direct spectrofluorimetric method has not been reported for the analysis of this drug, possibly due to its low fluorescence intensity.

One strategy for the enhancement of fluorescence signals of poorly fluorescent compounds is the use of organized media such as cyclodextrins (CDs) and surfactant micelles [18]. Through the inclusion complex-forming ability of CDs, the luminescence properties of the complexed analytes can be significantly modified [19]. On the other hand, micelles are able to include selected molecules into their amphipathic compartments, altering the microenvironment of the molecule and, in many cases, improving its luminescence signals.

With the dual purpose of improving the fluorescence properties of GAL and developing a new method for its determination, the effect of CDs and micellar systems on the fluorescence intensity was investigated. The selected cyclodextrins were α-, β-, γ- and

* Corresponding author at: Universidad Nacional de Rosario, Facultad de Ciencias Bioquímicas y Farmacéuticas, Departamento de Química Analítica, Suipacha 531, 2000 Rosario, Santa Fe, Argentina.
*E-mail addresses:* escandar@iquir-conicet.gov.ar, gmescandar@hotmail.com (G.M. Escandar).

0039-9140/$ – see front matter © 2010 Elsevier B.V. All rights reserved.
doi:10.1016/j.talanta.2010.04.043

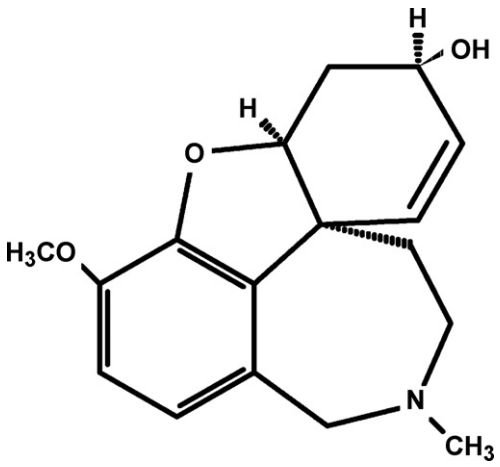


**Fig. 1.** Galantamine.

(2-hydroxy)propyl β-CDs, while micellar media included anionic, cationic and non-ionic surfactants. In order to determine the optimal working conditions, variables such as pH and temperature were also analyzed.

Although organized media could significantly increase the sensitivity of a luminescent method, the improvement in selectivity in complex matrices is more difficult to achieve because of the frequent spectral overlap from matrix interferences. In this context, certain second-order multivariate algorithms are useful tools for improving the selectivity of analytical methods, since they allow concentrations and spectral profiles of sample components to be extracted in the presence of any number of unsuspected constituents [20,21]. This property, named "second-order advantage", is especially convenient when analysts handle complex matrices, and it has been exploited in several real systems [22–26]. Therefore, the present quantitative analysis was carried out measuring excitation–emission fluorescence matrices (EEFMs) of GAL under optimal working conditions and in the presence of additional pharmaceuticals selected as interferences. The four investigated interferences were ibuprofen (IBU), acetyl salicylic acid (ASA), phenylephrine (PHE) and atropine (ATR), which have fluorescence spectra extensively overlapped with that of GAL, and maybe present in real water samples. The tested algorithms were parallel factor analysis (PARAFAC) [27], unfolded partial least-squares coupled to residual bilinearization (U-PLS/RBL) [28,29], and multidimensional partial least-squares [30] coupled to residual bilinearization (N-PLS/RBL). These algorithms, which achieve the second-order advantage, are appropriate for dealing with the data herein evaluated. A comparison between the employed algorithms is carried out and the feasibility of determining GAL in natural water samples is demonstrated.

## 2. Experimental

### 2.1. Apparatus

Fluorescence measurements were carried out on a PerkinElmer (Llantrisant, United Kingdom) LS 55 luminescence spectrometer equipped with a xenon discharge lamp, using a 1.00 cm quartz cell, 5 nm of excitation and emission slit widths, exciting at 230 nm and obtaining the fluorescence emission at 310 nm. The photomultiplier tube (PMT) voltage was set at 650 V. The data matrices were collected varying the excitation wavelength between 220 and 258 nm each 2 nm, and registering the emission spectra from 290 to 380 nm each 0.5 nm. Thus, the EEFMs were of size $20 \times 182$. The fluorescence measurements were made using a thermostated cell holder and a Lauda (Frankfurt, Germany) ALPHA RA8 thermostatic bath. The pH of solutions was measured with an Orion (Massachusetts, United States) 410 A potentiometer equipped with a Boeco (Hamburg, Germany) BA 17 combined glass electrode. Absorbance measurements were obtained with a PerkinElmer (Waltham, Massachusetts, USA) Lambda 20 spectrophotometer.

### 2.2. Reagents and solutions

All reagents were of high-purity grade and used as received. Galantamine hydrobromide, polyoxyethylene(23) dodecanol (Brij 35), hexadecyltrimethylammonium bromide (HTAB), sodium dodecylbenzenesulfonate (SDBS) and β-cyclodextrin (β-CD) were purchased from Sigma–Aldrich (Milwaukee, WI, USA). Hexadecyltrimethylammonium chloride (HTAC) and decyltrimethylammonium bromide (DeTAB) were provided by Fluka (Buchs, Switzerland). Sodium dodecylsulfate (SDS) was obtained from Merck (Darmstadt, Germany). α- and γ-cyclodextrins (α-CD and γ-CD) and (2-hydroxy)propyl β-cyclodextrin (HP-β-CD) were acquired from Cyclolab (Budapest, Hungary). Ibuprofen, acetyl salicylic acid, phenylephrine and atropine were obtained from Laboratory of Pharmaceutical Quality Control (Faculty of Biochemistry and Biological Sciences, National University of Litoral, Argentina).

A 200 $\mu g\,mL^{-1}$ stock solution of GAL was prepared in ultrapurified water (from a Millipore system) and stored in a dark flask at 4 °C. In these conditions, this solution was stable for at least two months.

### 2.3. Influence of cyclodextrin and surfactant concentrations

Taking into account that the aqueous solubility of β-CD is much lower than that of the rest of the analyzed CDs, two different strategies were implemented to study their effect on the fluorescence spectrum of GAL. For the β-CD system, suitable amounts of the stock solution of this CD were added to 2.00 mL volumetric flasks containing 0.5 $\mu g\,mL^{-1}$ GAL, in order to obtain final β-CD concentrations between 0 and 0.0090 mol $L^{-1}$. The samples were then completed to the mark with water and homogenized. Subsequently, fluorescence spectra were measured for each of the solutions. On the other hand, for the α-, γ- and HP-β-CD systems, 2.00 mL of 0.5 $\mu g\,mL^{-1}$ GAL were added with increasing aliquots of solutions containing each CD and 0.5 $\mu g\,mL^{-1}$ GAL, in order to avoid analyte dilution. After each addition, the fluorescence spectrum was measured. With the aim of subtracting the corresponding blank signals, these experiences were also performed without GAL.

For evaluating the effect of each surfactant concentration on the fluorescence signal of GAL, 2.00 mL of 0.5 $\mu g\,mL^{-1}$ GAL were spiked with increasing volumes of each of the detergent solutions containing 0.5 $\mu g\,mL^{-1}$ GAL. After each addition, the fluorescence spectrum was registered.

### 2.4. Influence of the pH

Both spectrophotometric and spectrofluorimetric titration experiments were conducted on acidified (pH ~ 2) solutions containing 5.0 and 0.5 $\mu g\,mL^{-1}$ of GAL, respectively, for solutions with and without the presence of SDS at its optimal concentration. The general procedure involves the addition of small aliquots of 0.05 or 1.0 mol $L^{-1}$ NaOH to 25.00 mL of the stirred original solution, in order to obtain small pH increments. As each new pH point was reached, the corresponding spectrum was acquired by extracting 2 mL of solution from the vessel, which were then restored, until pH ~ 12 was achieved. At the end of the titration, approximately 20 spectra were recorded for every experiment, which were processed by means of the PKFIT program [31], useful to obtain deprotonation constants from multi-wavelength spectroscopic pH titration data.

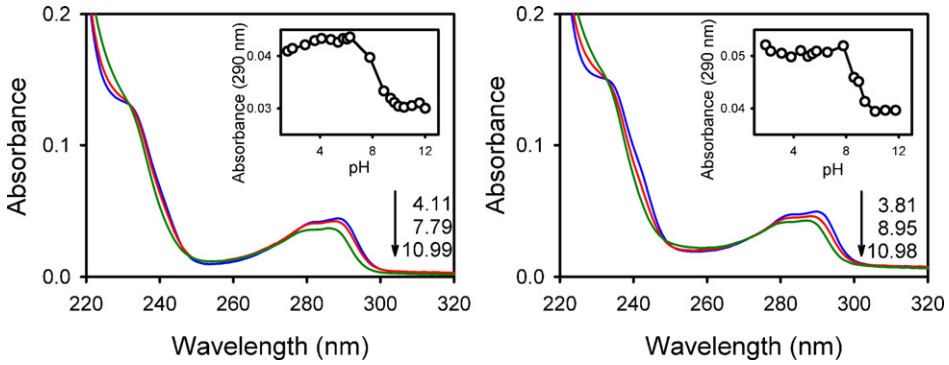


**Fig. 2.** (A) Absorption spectra of GAL alone and (B) in the presence of sodium dodecylsulfate (SDS) at the indicated pH values. The insets show the absorbance at 290 nm as a function of pH. $C_{GAL}$ = 0.5 μg mL$^{-1}$, $C_{SDS}$ = 0.05 mol L$^{-1}$.

### 2.5. Chemometric analysis coupled to EEFMs

#### 2.5.1. Theory

A brief description of the applied algorithms is given as Supplementary information.

#### 2.5.2. Calibration, validation and test samples

A calibration set of 7 samples was prepared by transferring appropriate aliquots of stock solution of GAL and 200 μL of 0.5 mol L$^{-1}$ SDS to 2.00 mL to volumetric flasks and completing to the mark with water. The final concentrations between 0.0 and 333 ng mL$^{-1}$ were included in the known linear fluorescence-concentration range. No attempts were made to establish the upper concentration of the linear range since the goal was to detect low concentrations of GAL.

A 12-sample validation set was built considering different concentrations of GAL than those used for calibration and following a random design.

Taking into account that in natural water samples it is likely to found GAL in the presence of other compounds, a test set of 12 samples was prepared having concentrations of GAL between 0.0 and 100 ng mL$^{-1}$ as well as 98.7, 512, 90.8 and 474 ng mL$^{-1}$ of IBU, ASA, PHE and ATR, respectively. These concentrations were selected taking into account they are high and likely to be on the order of the concentrations found in contaminated natural waters. In the cases of ASA and ATR, the concentrations were about 500 ng mL$^{-1}$ in order to enhance their fluorescence signals.

#### 2.5.3. Real samples

Real samples were prepared by spiking river, tap and well water with standard solution of GAL to have three different concentration levels. Besides, the interferences IBU, ASA, PHE and ATP were incorporated at the concentrations mentioned above. Then, the solutions were passed through Whatman filter papers (London, England). Before recording the EEFMs, 200 μL of 0.5 mol L$^{-1}$ SDS were added to 2.00 mL volumetric flasks and completed to the mark with each sample. This procedure was performed in duplicate.

The GAL concentrations in real samples were corroborated analyzing aliquots of the same investigated samples by an HPLC method with fluorescence detection ($\lambda_{ex}/\lambda_{em}$ = 230/310 nm) following the chromatographic conditions suggested in the literature [10].

#### 2.5.4. Software

All employed algorithms were implemented in MATLAB 7.6 [32]. Those for applying PARAFAC are available in the Internet thanks to Bro [33]. Both N-PLS/RBL and U-PLS/RBL were implemented by means of the integrated chemometric toolbox MVC2 [34], which also provides access to a variety of second-order multivariate methodologies including PARAFAC. The program is available from the authors on request or in www.chemometry.com. Deprotonation constants were determined using the PKFIT program [31], which is based on a full-spectrum least-squares procedure. It can also be obtained from the authors on request.

## 3. Results and discussion

### 3.1. Spectral characteristics of GAL

Previous to the quantitative study, and in order to establish adequate working conditions, both the absorption and fluorescence characteristics of GAL and its acid–base behavior were evaluated.

The absorption spectrum of GAL shows a wide band between 270 and 300 nm and a more intense shoulder located at 233 nm (Fig. 2A). From pH titration multi-wavelength spectrophotometric data, the deprotonation constant of GAL in the ground state could be determined. Although this constant was calculated using the whole spectrum, with the purpose of showing the variation of the absorbance vs. pH, the changes in the absorbance at a fixed wavelength (290 nm) is illustrated in the insert of Fig. 2A. The obtained value [p$K_a$ = 8.4 (0.1)] is similar to that informed in literature (p$K_a$ = 8.32, Ref. [35]).

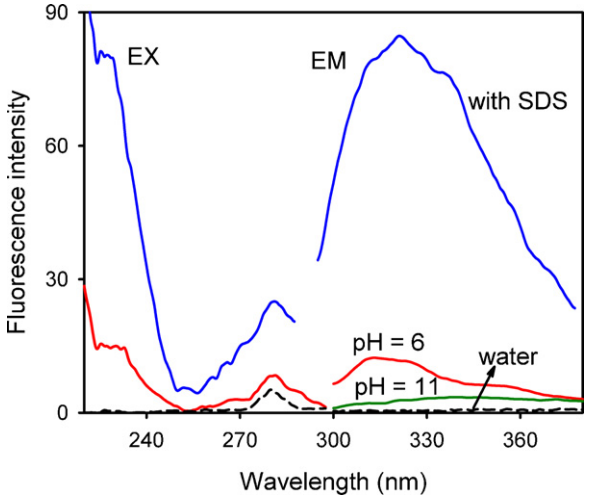


**Fig. 3.** Excitation (EX) and emission (EM) fluorescence spectra for GAL alone at pH = 6 (red solid line) and pH = 11 (green solid line), and in the presence of sodium dodecylsulfate (SDS) [blue solid line; neutral pH]. The blank (water) signal is indicated with black dotted lines. $C_{GAL}$ = 0.5 μg mL$^{-1}$, $C_{SDS}$ = 0.05 mol L$^{-1}$, $\lambda_{ex/em}$ = 230/310 nm. (For interpretation of the references to color in this figure caption, the reader is referred to the web version of the article.)

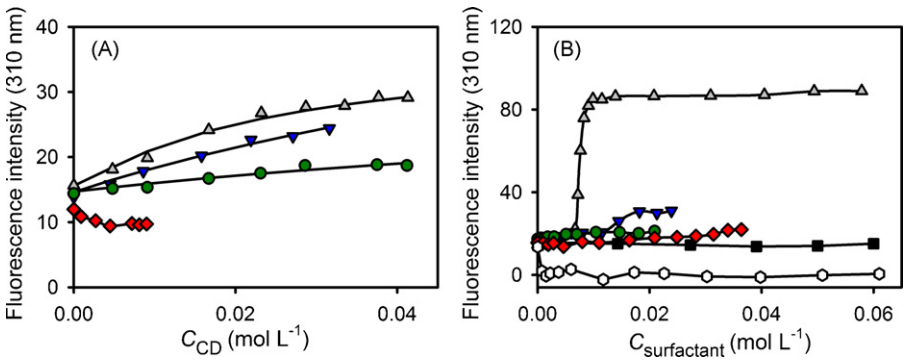


**Fig. 4.** Influence of α-CD (gray triangle up), β-CD (red diamond), γ-CD (green circle) and HP-β-CD (blue triangle down) concentrations (A) and SDBS (white circle), DeTAB (black square), HTAC (red diamond), HTAB (green circle), Brij 35 (blue triangle down) and SDS (gray triangle up) concentrations (B) on the fluorescence emission of GAL at neutral pH. The solid lines in α-, HP-β- and γ-CD systems are the non-linear fit of the data assuming the formation of 1:1 complexes. $C_{GAL}$ = 0.5 μg $mL^{-1}$. (For interpretation of the references to color in this figure caption, the reader is referred to the web version of the article.)

Besides, Fig. 3 shows fluorescence spectra of GAL under different conditions. From this figure several conclusions can be made: (i) a rather weak native fluorescence emission is obtained at 310 nm, (ii) the fluorescence intensity is higher when GAL remains in its protonated form (pH < 8), (iii) the excitation band at about 230 nm (coincident with the maximum absorption at this wavelength) is high and more suitable for quantitative determinations, and (iv) the excitation band at 280 nm, usually employed in HPLC techniques with fluorescence detection [2,12], is coincident with a Raman dispersion when the emission is obtained at 310 nm and, therefore, inconvenient for analytical purposes.

From the changes of fluorescence spectra as a function of pH (not shown), the deprotonation constant value in the excited state was calculated. The obtained value [$pK_{a'}$ = 8.3 (0.1)], similar to that obtained through the spectrophotometric assay, indicates that the fluorescence decay process is faster than the deprotonation in the excited state [36].

### 3.2. Influence of organized media

It is relevant to note that the rather weak native fluorescence of GAL would not allow its quantitation at low concentrations, i.e. at ng $mL^{-1}$ units which, in principle, are the pharmaceutical levels expected to be found in environmental water samples [5,6]. Therefore, several organized media were checked as enhancers of the GAL fluorescence.

The three major cyclodextrins, α-, β-, and γ-CDs, which comprise six, seven, and eight glucose units, respectively, and the derivative hydroxypropylated β-CD (HP-β-CD) were investigated. In Fig. 4A it is displayed the intensities of the fluorescence emissions of GAL at different concentrations of the studied CDs. As can be appreciated, β-CD does not modify the fluorescence properties of GAL, and therefore this CD is not useful for our purposes. The remaining CDs modify the fluorescence signal in different degrees. Although α-CD showed the best fluorescence enhancement, this improvement is not high enough to reach the low GAL concentrations assayed.

From the α-, γ- and HP-β-CDs profiles shown in Fig. 4A, the 1:1 association constants were determined by applying non-linear regression analysis [37]. The obtained values, 25 (6), 11 (5) and 19 (4) $mol^{-1}$ L for α-, γ- and HP-β-CD complexes, respectively, suggest very weak interactions for the three complexes. The values for both α- and γ-CD agree with those previously reported using other techniques of inclusion constant determination: 23.90 $mol^{-1}$ L and 33.98 $mol^{-1}$ L for the two GAL enantiomers and α-CD [38], and 5 $mol^{-1}$ L for γ-CD [16]. The previously reported value for HP-β-CD ($K$ = 8 $mol^{-1}$ L, Ref. [16]) slightly differs from our calculation.

The effect produced by micelles on the fluorescence intensity of GAL was also evaluated by keeping a constant concentration of GAL and increasing the surfactant concentrations (Fig. 4B). Among the studied surfactants, SDS at concentrations higher than 0.01 mol $L^{-1}$ produced the best results, with a signal enhancement factor of 6.1 [39]. The micelles formed by HTAC, HTAB and Brij35 produced a slight increase in the GAL fluorescence signal, while DeTAB did not modify the signal, and SDBS showed a quenching effect. Therefore, to ensure stable and high fluorescence signals, 0.05 mol $L^{-1}$ SDS solution was selected as auxiliary reagent for quantitative determinations (see Fig. 3).

Since micelles can modify the acid–base properties of a compound in both ground and excited states [39], the deprotonation constant value of GAL in the presence of SDS was evaluated by spectrophotometry and spectrofluorimetry. In Fig. 2B, it can be appreciated that the addition of SDS does not produce significant changes in the absorption spectrum of GAL. The fact that the deprotonation value obtained by spectrophotometric titration [$pK_a$ = 9.3 (0.3)] is higher than that the one previously calculated in the absence of SDS [$pK_a$ = 8.4, see above] may be explained in terms of the stabilization of the protonated form of GAL by ion pair formation between this positively charged structure and the anionic surfactant. On the other hand, the acidity constant of GAL in the SDS system evaluated from spectrofluorimetric titration, with a value of $pK_{a'}$ = 9.2 (0.4), is similar to that obtained by spectrophotometry, indicating again that the fluorescence decay process of GAL in the micellar medium is faster that the deprotonation in the excited state. It is necessary to point out that the fluorescence emission intensity in the SDS system is higher at pH below 8 and, therefore, the work was carried out in micellar aqueous solutions, without the necessity of using buffer solutions.

Finally, it was corroborated that a temperature decrease does not significantly modify the fluorescence signals of the studied system in both the presence and absence of micellar media. Therefore, the experiments were conducted at 20 °C.

### 3.3. Multivariate calibration results

The quantitative study was carried out by chemometric analysis with three algorithms which achieve the second-order advantage, namely, PARAFAC, U-PLS/RBL and N-PLS/RBL. On the basis of the experiments described above, the conditions applied for the determination of GAL by chemometric analysis are those given in Table 1.

#### 3.3.1. Validation and test samples

In order to build a second-order calibration model, EEFMs were recorded for the calibration samples. In Fig. 5A a three-dimensional

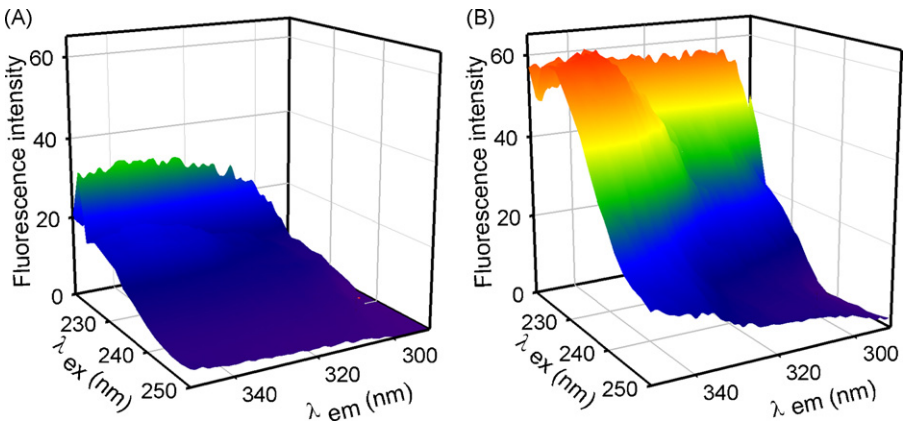


**Fig. 5.** Three-dimensional plots for excitation–emission fluorescence matrices corresponding to a typical validation sample containing 45 ng mL$^{-1}$ GAL (A) and a typical test sample containing 45 ng mL$^{-1}$ GAL, 98.7 ng mL$^{-1}$ IBU, 512 ng mL$^{-1}$ ASA, 90.8 ng mL$^{-1}$ PHE and 474 ng mL$^{-1}$ ATR (B).

**Table 1**
Instrumental and chemical parameters for the chemometric analysis.

| | Values |
|---|---|
| Selected excitation range (nm) | 220–250 |
| Selected emission range (nm) | 290–350 |
| Slits (excitation/emission) (nm) | 5/5 |
| Photomultiplier voltage (V) | 650 |
| $C_{SDS}$ (mol L$^{-1}$) | 0.05 |
| pH | ~7 |
| Temperature (°C) | 20 |

plot of the EEFM is shown for a typical studied sample in the appropriately selected wavelength ranges.

While the number of responsive components to be included in the PARAFAC model was selected by the so-called core consistency analysis [40], the number of optimum latent variables for both U- and N-PLS was obtained through leave-one-sample-out cross-validation [41]. In all cases, the number of components in validation samples was 2, attributed to the analyte and the background signals.

In Fig. 6A–C the prediction results corresponding to the application of PARAFAC, U-PLS and N-PLS, respectively, are shown to the same set of 12 validation samples. In Fig. 6E the ellipses of the EJCR analyses are shown for the slope and intercept of the corresponding plots. While the ellipses corresponding to PARAFAC and U-PLS include the theoretically expected point (1,0) suggesting a high-quality prediction, the one corresponding to N-PLS does not include this point, indicating a deficient accuracy. This latter fact demonstrates that in the system under study it is not appropriate to maintain the tridimensional nature of the data for the quantitative analysis in order to successfully quantitate the analyte.

Comparison of the statistical results obtained from U-PLS with those obtained by applying both N-PLS and PARAFAC to the validation samples (Table 2) shows that the former renders significantly better results.

With the purpose of analyzing the potentiality of the evaluated second-order algorithms, the determination of GAL was carried out in the presence of selected pharmaceuticals with either direct or indirect relationship with Alzheimer disease (IBU [42,43], ASA [44], PHE [45] and ATR [46,47]), which overlap their spectra with GAL, and could be concomitantly present in the same samples. Fig. 5B shows a three-dimensional plot of the EEFM for a typical test sample containing GAL and the four interferences, under the applied working conditions and in the selected wavelength ranges. Fig. 7 shows the individual contour plots of the EEFMs for these interferences. For clarity these latter plots are shown separately.

Twelve test samples containing the studied analyte and IBU, ASA, PHE and ATR were prepared and evaluated with PARAFAC, U-PLS/RBL and N-PLS/RBL algorithms. The selection of PARAFAC factors for these samples was also carried out through the analysis of the core consistency. The results obtained established that the number of total components required by PARAFAC in samples with the studied interferences was three. Unfortunately, the GAL prediction ability of PARAFAC in samples with interferences was worse than that obtained in the validation samples (data not reported).

On the other hand, when U- and N-PLS/RBL algorithms were applied to the test samples, in addition to the number of latent variables estimated for the calibration set, these samples required the introduction of the RBL procedure with four unexpected components in most cases. While N-PLS/RBL rendered bad results (which were not considered further) the U-PLS/RBL predictions were in good agreement with the corresponding nominal values (Fig. 6D).

**Table 2**
Statistical results for GAL in validation samples and in samples with IBU, ASA, PHE and ATR as interferences, using the indicated chemometric algorithms.

| | $m$[a] | $h$[a] | $R$[b] | RMSEP[c] | REP[d] | LOD[e] | LOQ[f] |
|---|---|---|---|---|---|---|---|
| *Validation samples*[g] | | | | | | | |
| PARAFAC | 1.2 | −19 | 0.984 | 16 | 10 | 3 | 9 |
| N-PLS | 1.2 | −13 | 0.978 | 16 | 10 | 4 | 12 |
| U-PLS | 1.1 | −9 | 0.993 | 8 | 5 | 4 | 12 |
| *Samples with interferences*[g] | | | | | | | |
| U-PLS/RBL | 0.9 | 2.9 | 0.989 | 6 | 4 | 8 | 24 |

[a] $m$ and $h$ are the slope and intercept of the linear regression of predicted vs. nominal concentration, respectively.
[b] Correlation coefficients of the linear regressions of predicted vs. nominal concentration.
[c] RMSEP, root-mean-square error of prediction in ng mL$^{-1}$.
[d] REP, relative error of prediction in %.
[e] LOD, limit of detection in ng mL$^{-1}$ calculated according to Ref. [25].
[f] LOQ, limit of quantitation in ng mL$^{-1}$ calculated as (10/3.3) × LOD.
[g] Number of samples = 12.

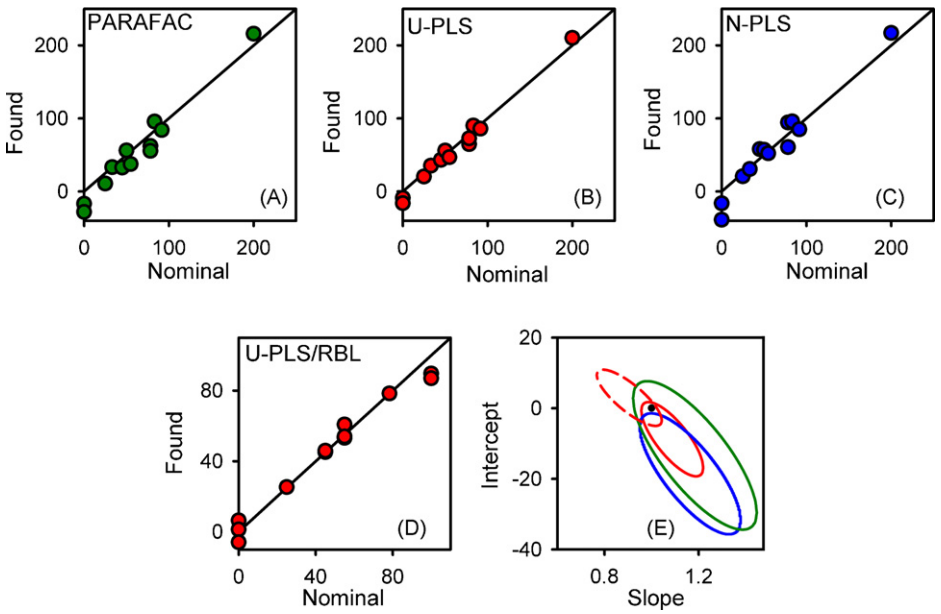


**Fig. 6.** Plots of GAL predicted concentrations in validation samples as a function of the nominal values using (A) PARAFAC, (B) U-PLS (C) N-PLS, and (D) in samples with interferences using U-PLS/RBL. (E) Elliptical joint regions (at 95% confidence level) for the slope and intercept of the regression of PARAFAC (green solid line), U-PLS (red solid line), N-PLS (blue solid line) and U-PLS/RBL (red dashed line) results. Black point marks the theoretical (intercept = 0, slope = 1) point. (For interpretation of the references to color in this figure caption, the reader is referred to the web version of the article.)

Both the EJCR for the slope and intercept of the above plot (Fig. 6E, red dashed line) and the statistical results shown in Table 2, with very satisfactory values for RMSEP and REP, support this conclusion. These results are not completely surprising since in previous works [24,25,48,49], U-PLS/RBL has already demonstrated to be superior to N-PLS/RBL, especially when there is a strong spectral overlapping between the analyte and interferences. Further studies should be made in order to gain a deeper insight into this interesting aspect of second-order multivariate calibration.

The LODs obtained by U-PLS/RBL in the absence (4 ng mL$^{-1}$) and in the presence of interferences (8 ng mL$^{-1}$), are very acceptable taking into account that a simple methodology is applied to complex samples. A wide range of limits of detection have been previously informed for GAL in different matrices: 11 ng mL$^{-1}$ (HPLC with fluorescence detection in plasma samples, Ref. [12]) and 184 ng mL$^{-1}$ (flow injection determination by immobilised acetylcholinesterase inhibition, Ref. [7]). A chiral HPLC method with UV detection allowed a limit of detection of 210 ng mL$^{-1}$ for the *R*-enantiomer in pharmaceutical formulations [14]. After repeated liquid–liquid extraction, a GAL level of 5 ng mL$^{-1}$ was the minimum detectable concentration in serum by HPLC with UV detection [8]. Following liquid–liquid extractions of human plasma samples,

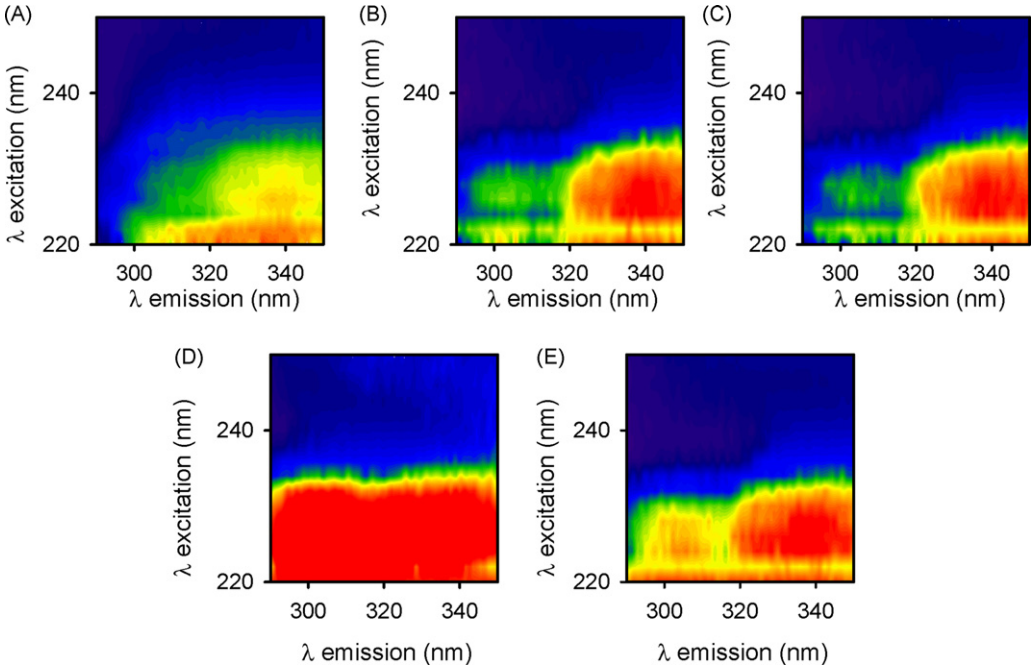


**Fig. 7.** Two-dimensional contour plots of the excitation–emission fluorescence matrices for samples containing the studied analyte and interferences, all in the presence of SDS 0.05 mol L$^{-1}$. GAL (A), ATR (B), ASA (C), IBU (D) and PHE (E). $C_{GAL}$ = 60 ng mL$^{-1}$; $C_{ATR}$ = 474 ng mL$^{-1}$; $C_{ASA}$ = 512 ng mL$^{-1}$; $C_{IBU}$ = 98.7 ng mL$^{-1}$; $C_{PHE}$ = 90.8 ng mL$^{-1}$.

**Table 3**
Recovery study of GAL in spiked water samples in the presence of IBU, ASA, PHE and ATR.[a].

| | Nominal ($ng\,mL^{-1}$) | Found ($ng\,mL^{-1}$)[b] | |
|---|---|---|---|
| | | EEFM–U-PLS/RBL | HPLC |
| River water[c] | 30.0 | 32 (9) [107] | 29 (2) [97] |
| | 72.0 | 65 (4) [90] | 72 (1) [100] |
| | 108 | 106 (2) [98] | 109 (1) [101] |
| River water[d] | 30.0 | 33 (9) [110] | 35 (1) [117] |
| | 72.0 | 71 (2) [92] | 74 (2) [103] |
| | 108 | 108 (3) [100] | 106 (1) [98] |
| Tap water[e] | 30.0 | 31 (1) [103] | 34 (2) [113] |
| | 72.0 | 71 (3) [99] | 73 (1) [101] |
| | 108 | 103 (4) [95] | 110 (1) [102] |
| Well water[f] | 30.0 | 27 (3) [90] | 31 (1) [103] |
| | 72.0 | 80 (3) [111] | 71 (1) [99] |
| | 108 | 108 (9) [100] | 110 (1) [102] |

[a] $C_{IBU} = 98.7\,ng\,mL^{-1}$, $C_{ASA} = 512\,ng\,mL^{-1}$, $C_{PHEN} = 90.8\,ng\,mL^{-1}$ and $C_{ATR} = 474\,ng\,mL^{-1}$.
[b] Experimental standard deviation of duplicates, in the last significant figure, in parentheses. The recoveries (in square brackets) are based on the added amounts.
[c] Salado River (Santa Fe, Argentina).
[d] Coronda River (Sauce Viejo, Argentina).
[e] From Santa Fe City (Santa Fe, Argentina).
[f] From Colastiné City (Santa Fe, Argentina).

GAL was determined by HPLC–MS and HPLC–MS–MS with limits of quantification of 0.5 and $1.00\,ng\,mL^{-1}$ respectively [13,10]. GC–MS and non-aqueous capillary electrophoresis methods were applied to the quantification of galantamine in the bulbs of *Narcissus* species, with LODs of 1800 and $2000\,ng\,mL^{-1}$, respectively [15]. A method based on solvent extraction and HPLC with UV detection allowed the determination of GAL in plants at levels of about $12{,}800\,ng\,mL^{-1}$ [11].

In conclusion, we can assert that taking into account the instrumental simplicity of the proposed method and that preconcentration steps were not performed, the levels of measured concentrations are more than satisfactory.

### 3.3.2. Real water samples

According to the obtained results with artificial samples, U-PLS/RBL was selected as the algorithm to be applied to real samples. Because of the analyzed water samples were found to be free from GAL residues, spiked samples were prepared and a recovery study was performed. In addition to inorganic and organic compounds which may be present in each type of water, the four selected pharmaceuticals were also incorporated to the samples.

Table 3 summarizes the results obtained from duplicate analyses of three different GAL levels in real matrices. The equivalence among the recoveries demonstrates the ability of U-PLS/RBL to cope with interferences from the concomitants in the real samples. The values obtained are statistically comparable to those provided by a reference method when a paired Student *t*-test is applied at a 95% confidence level. The calculated *t*-coefficient [$t_{(0.05,23)} = 1.60$] compares favourably with the tabulated value [$t_{crit(0.05,23)} = 2.07$], suggesting that the proposed method is appropriate for the determination of GAL.

## 4. Conclusions

The relatively weak fluorescence of GAL is significantly enhanced using micellar medium formed by SDS. The combination of excitation–emission fluorescence matrices of GAL in the presence of SDS with a selected second-order algorithm (U-PLS/RBL) allowed the successful determination of this acetylcholinesterase inhibitor in samples with and without spectral interferences. While PARAFAC yield good results in validation samples, a deficient recovery is provided when foreign compounds are present, which significantly overlap their spectra with the analyte. On the other hand, N-PLS/RBL, which is similar to the unfolded U-PLS method but original data matrices are not unfolded, yields inadequate results in both types of samples. The developed method is very simple, possesses high selectivity and is able to determine GAL at levels of the $ng\,mL^{-1}$ without the necessity to apply either extraction or pre-concentration steps.

## Acknowledgments

Universidad Nacional de Rosario, CONICET (Consejo Nacional de Investigaciones Científicas y Técnicas, Project PIP 1950), and ANPCyT (Agencia Nacional de Promoción Científica y Tecnológica, Project PAE-22204) are gratefully acknowledged for financial support. MJC thanks CONICET for a fellowship, and RQA thanks CNPq-Brazil for a scholarship.

## Appendix A. Supplementary data

Supplementary data associated with this article can be found, in the online version, at doi:10.1016/j.talanta.2010.04.043.

## References

[1] C.J. Hilmas, M.J. Poole, K. Finneran, M.G. Clark, P.T. Williams, Toxicol. Appl. Pharm. 240 (2009) 166.
[2] G.S.J. Mannens, C.A.W. Snel, J. Hendrickx, T. Verhaeghe, L. Le Jeune, W. Bode, L. Van Beijsterveldt, K. Lavrijsen, J. Leempoels, N. Van Osselaer, A. Van Peer, W. Meuldermans, Drug Metab. Dispos. 30 (2002) 553.
[3] R. Andreozzi, R. Marotta, G. Pinto, A. Pollio, Water Res. 36 (2002) 2869.
[4] K. Reddersen, T. Heberer, J. Sep. Sci. 26 (2003) 1443.
[5] M. Gros, M. Petrović, D. Barceló, Anal. Bioanal. Chem. 386 (2006) 941.
[6] S.D. Richardson, Anal. Chem. 81 (2009) 4645.
[7] T. Ghous, A. Townshend, Anal. Chim. Acta 372 (1998) 379.
[8] H.A. Claessens, M. Van Thiel, P. Westra, A.M. Soeterboek, J. Chromatogr. 275 (1983) 345.
[9] J. Tencheva, I. Yamboliev, Z. Zhivkova, J. Chromatogr. 421 (1987) 396.
[10] T. Verhaeghe, L. Diels, R. de Vries, M. De Meulder, J. de Jong, J. Chromatogr. 789B (2003) 337.
[11] N.R. Mustafa, I.K. Rhee, R. Verpoorte, J. Liq. Chromatogr. R. T. 26 (2003) 3217.
[12] J. Maláková, M. Nobilis, Z. Svoboda, M. Lísa, M. Holčapek, J. Květina, J. Klimeš, V. Palička, J. Chromatogr. B 853 (2007) 265.
[13] R.V.S. Nirogi, K.N. Vishwottam, M. Koteshwara, M. Santosh, J. Chromatogr. Sci. 45 (2007) 97.
[14] V. Ravinder, S. Ashok, A.V.S.S. Prasad, G. Balaswamy, Y.R. Kumar, B.V. Bhaskar, Chromatographia 67 (2008) 331.
[15] R. Gotti, J. Fiori, M. Bartolini, V. Cavrini, J. Pharm. Biomed. Anal. 42 (2006) 17.
[16] A. Rizzi, R. Schuh, A. Brückner, B. Cvitkovich, L. Kremser, U. Jordis, J. Fröhlich, B. Küenburg, L. Czollner, J. Chromatogr. B 730 (1999) 167.
[17] L. Pokorna, A. Revilla, J. Havel, J. Patocka, Electrophoresis 20 (1999) 1993.
[18] J.J. Santana Rodríguez, R. Halko, J.R. Betancort Rodríguez, J.J. Aaron, Anal. Bioanal. Chem. 385 (2006) 525.
[19] J. Szejtli, Pure Appl. Chem. 76 (2004) 1825.
[20] K.S. Booksh, B.R. Kowalski, Anal. Chem. 66 (1994) 782A.
[21] Å. Rinnan, J. Riu, R.J. Bro, J. Chemom. 21 (2007) 76.
[22] G.N. Piccirilli, G.M. Escandar, Analyst 131 (2006) 1012.
[23] D. Bohoyo Gil, A. Muñoz de la Peña, J.A. Arancibia, G.M. Escandar, A.C. Olivieri, Anal. Chem. 78 (2006) 8051.
[24] G.M. Escandar, N.M. Faber, H.C. Goicoechea, A. Muñoz de la Peña, A.C. Olivieri, R.J. Poppi, Trends Anal. Chem. 26 (2007) 752.
[25] S.A. Bortolato, J.A. Arancibia, G.M. Escandar, Anal. Chem. 80 (2008) 8276.
[26] S.A. Bortolato, J.A. Arancibia, G.M. Escandar, Anal. Chem. 81 (2009) 8074.
[27] R. Bro, Chemom. Intell. Lab. Syst. 38 (1997) 149.
[28] J. Öhman, P. Geladi, S. Wold, J. Chemom. 4 (1990) 135.
[29] A.C. Olivieri, J. Chemom. 19 (2005) 253.
[30] R. Bro, J. Chemom. 10 (1996) 47.
[31] G.A. Ibañez, G.M. Escandar, A.C. Olivieri, Chem. Educator 12 (2007) 22.
[32] MATLAB 7.1, The MathWorks Inc., Natick, Massachussets, USA, 2005.
[33] http://www.models.kvl.dk/source.
[34] A.C. Olivieri, W. Hai-Long, Y. Ru-Qin, Chemom. Intell. Lab. Syst. 96 (2009) 246.
[35] A.L. Harvey, Pharmac. Ther. 68 (1995) 13.
[36] S.G. Schulman, Acid–base chemistry of excited singlet states, in: E.L. Wehry (Ed.), in: Modern Fluorescence Spectroscopy, vol. 2, Plenum Publishing Corporation, New York, 1976 (Chapter 6).

[37] A. Muñoz de la Peña, I. Durán-Merás, F. Salinas, I.M. Warner, T.T. Ndou, Anal. Chim. Acta 255 (1991) 351.
[38] M. Sun, X. Liu, L. Yan, G. Luo, Y. Zhao, J. Mol. Model 9 (2003) 419.
[39] E. Pramauro, E. Pelizzetti, Surfactants in analytical chemistry. Applications of organized amphiphilic media, in: S.G. Weber (Ed.), in: Comprehensive AnalyticalChemistry, vol. 31, Elsevier, Wilson & Wilson's, Amsterdam, The Netherlands, 1996 (Chapter 4).
[40] R. Bro, H.L. Kiers, J. Chemom. 17 (2003) 274.
[41] D.M. Haaland, E.V. Thomas, Anal. Chem. 60 (1988) 1193.
[42] G.P. Lim, F. Yang, T. Chu, E. Gahtan, O. Ubeda, W. Beech, J.B. Overmier, K. Hsiao-Ashe, S.A. Frautschy, G.M. Cole, Neurobiol. Aging 22 (2001) 983.
[43] C. Babiloni, G.B. Frisoni, C. Del Percio, O. Zanetti, C. Bonomini, E. Cassetta, P. Pasqualetti, C. Miniussi, M. De Rosas, A. Valenzano, G. Cibelli, F. Eusebi, P.M. Rossini, Clin. Neurophysiol. 120 (2009) 709.
[44] G.A. Broe, D.A. Grayson, H.M. Creasey, L.M. Waite, B.J. Casey, H.P. Bennett, Arch. Neurol. 57 (2000) 1586.
[45] H. Hanyu, K. Hirao, S. Shimizu, H. Kanetaka, H. Sakurai, T. Iwamoto, Neurosci. Lett. 414 (2007) 174.
[46] E. Moor, E. Schirm, J. Jacsó, B.H.C. Westerink, Neuroscience 82 (1998) 819.
[47] Y. Goto, T. Niidome, H. Hongo, A. Akaike, T. Kihara, H. Sugimoto, Eur. J. Pharm. 583 (2008) 84.
[48] M.D. Borraccetti, P.C. Damiani, A.C. Olivieri, Analyst 134 (2009) 1682.
[49] A.C. Olivieri, Anal. Chem. 80 (2008) 5713.